Low temperature transport through a quantum dot: finite-U results and scaling behavior

D. Gerace, E. Pavarini, and L. C. Andreani

Istituto Nazionale per la Fisica della Materia and Dipartimento di Fisica "A. Volta", Università di Pavia, Via Bassi 6, 27100 Pavia, Italy

(February 6, 2008)

We calculate the conductance through a quantum dot weakly coupled to metallic leads, modeled by the spin-1/2 Anderson model with finite Coulomb repulsion U. We adopt the non-crossing approximation method in its finite-U extension (UNCA). Our results can be compared to those obtained with the exact numerical renormalization group method, and good agreement is found both in the high temperature (Coulomb blockade) and in the low temperature (Kondo) regime. We analyze the scaling properties of the low temperature conductance, and calculate the universal function which describes the electronic transport in the Kondo regime. Very good agreement with recent experimental results is found. Finally, we suggest a simple interpolating function which fits fairly well the calculated conductance in a broad temperature range.

PACS: 72.15.Qm, 73.23.-b, 73.63.Kv

I. INTRODUCTION

The Kondo effect, a phenomenon discovered in the late 30s in diluted magnetic alloys, plays a crucial role in the low temperature properties of many strongly correlated systems, such as Ce, Y and U compounds.[1] Very recently Kondo-like phenomena were also observed in the low-temperature transport properties of quantum dot devices,[2–9] opening new opportunities to control the Kondo effect experimentally, and starting a new field of research.[10]

A quantum dot device consists of a small sized quantum dot (QD) weakly connected by tunnel barriers to two electrodes, called source and drain. In this system the QD may be considered as an artificial atom, in which a well defined number of electrons, n, is confined. The energy required to add a new electron to the QD is $U = e^2/2C$, where C is the capacitance of the QD itself. The energy U is determined by the Coulomb repulsion between two electrons in the QD and thus it scales with the inverse of the dot dimensions. Therefore, in small sized QD, U is usually larger than the coupling to the leads. An important aspect of a QD device is that the energy of electrons in the dot can be tuned by a gate voltage. Increasing the gate voltage, the energy necessary to add a new electron decreases, eventually making the addition possible. Thus it was shown that, at low temperature, the transport of electrons through the QD is allowed only at those values of the gate voltage at which the state with n electrons is realized and that with $n+1$ electrons becomes suddenly energetically accessible (Coulomb blockade).[11,12]

The idea that Kondo-like phenomena should appear in such a system at very low temperature can be traced back to 1988. In that year it was recognized that the Anderson model, introduced in 1961 to describe a magnetic impurity in a metal,[13] could also be applied to a QD coupled to its leads.[14,15] Soon afterwards several theoretical studies have been devoted to analyze the properties of such a system (see e.g. Refs. 16–23). It was predicted that at very low temperature ($T \ll T_K$, where T_K is the Kondo temperature) a narrow peak should appear in the local density of states, close to the Fermi level. Thus, states belonging to opposite electrodes should mix easier than at high temperature ($T \gg T_K$), and the conductance should increase. In addition, the Kondo anomalies were predicted to appear only for odd n,[14–16] and thus only if the total spin of the electrons in the QD, S, is half integer. These predictions are now confirmed by several experimental results.[2–7] The Kondo temperature of QD devices is however very small (usually less than a few hundred mK) compared to the one of diluted magnetic alloys (usually a few K). Recently,[8,9] in some QD devices Kondo anomalies have been observed for even n as well; it is believed that these deviations from the even/odd n effect are related to the formation of integer spin states with $S \geq 1$.

In the present paper we will focus our attention on those QD devices for which the Kondo effect occurs *only* for odd n. The transport properties of such a QD device have been calculated by using many different approaches, such as the equations of motion method,[17] the non-crossing approximation (NCA)[19,20] and the exact numerical renormalization group (NRG) technique.[21–23] Within the NRG it was possible to calculate the conductance as a function of the gate voltage, and thus to obtain – in the case $S = 1/2$ – the even/odd effect in very good agreement with experimental results. Similar results were also obtained with the approximate equations of motion method and with the NCA. The latter

method[24,25] was applied to low temperature transport of a QD in the infinite U limit and thus the even/odd alternation effect was obtained[20] for n switching from $n = 0$ to $n = 1$.

Even if approximated, the NCA can be easily extended to models in which the realistic levels structure of the QD is kept into account (i.e. in the presence of several levels and possibly of an external magnetic field), thus becoming a very convenient method for a direct comparison to transport properties of real QD devices. As a matter of fact, the NCA was used with success to study, e.g., orbital degeneracy effects in diluted magnetic alloys.[24–26] However, in the case of QD devices, it is first necessary to go beyond the $U \longrightarrow \infty$ condition, which does not account for the even/odd effect for all values of n.

In the present work we apply the finite-U NCA method[27] to the QD device system, modeled by the spin-1/2 Anderson model. We calculate the conductance as a function of the position of the QD level, and study the system in the empty orbital, mixed valence and Kondo regimes. Our results are in good agreement with the exact numerical renormalization group ones. In particular, we obtain the correct behavior of the conductance both in the high temperature regime, $T \gg T_K$, in which the conductance shows the Coulomb blockade peaks, and the low temperature regime, $T < T_K$, where the conductance increases for odd n due to the Kondo effect.

The paper is organized as follows. In section II we describe the model Hamiltonian and give a short introduction to the finite-U NCA. In section III we show and discuss the numerical results, in particular the linear-response conductance, which we compare to exact results and to experimental data. In section IV we study the scaling behavior of the conductance as a function of temperature, and we suggest an empirical formula which is valid both in the Fermi-liquid and in the $T \sim T_K$ temperature regime, where the conductance has a logarithmic behavior.

II. MODEL AND METHOD

A. Hamiltonian

In order to describe a quantum dot (QD) coupled with its leads we adopt the Anderson Hamiltonian[15]

$$H = \sum_{(\mathbf{k},\sigma)\in S,D} \varepsilon_{\mathbf{k}}\, c^\dagger_{\mathbf{k}\sigma} c_{\mathbf{k}\sigma} + \varepsilon_0 \sum_\sigma d^\dagger_\sigma d_\sigma + U\, n_{d\uparrow} n_{d\downarrow} + \sum_{(\mathbf{k},\sigma)\in S,D} \left(V_{\mathbf{k}\sigma} c^\dagger_{\mathbf{k}\sigma} d_\sigma + h.c. \right). \quad (1)$$

Here $c^\dagger_{\mathbf{k}\sigma}$ ($c_{\mathbf{k}\sigma}$) creates (destroys) a conduction electron with momentum $\mathbf{k}$ and spin σ in one of the two leads, which we label with S (source) and D (drain); $d^\dagger_\sigma$ (d_σ) creates (destroys) an electron with spin σ on the quantum dot; ε_0 is the energy of a single electron localized on the QD and U is the Coulomb interaction among electrons in the dot; $n_{d\sigma} = d^\dagger_\sigma d_\sigma$ is the number of electrons operator for a given spin in the QD; $V_{\mathbf{k}\sigma}$ is the hybridization between the leads and the QD states, whose modulus is supposed to be $\mathbf{k}$-independent, with $|V_{\mathbf{k}\sigma}| = V_{S(D)}$ for $(\mathbf{k},\sigma) \in S(D)$. The lead-dot coupling strengths are given by

$$\Gamma_{S(D)} \equiv \pi V^2_{S(D)} \sum_{\mathbf{k}} \delta(\varepsilon - \varepsilon_{\mathbf{k}}). \quad (2)$$

It was shown[15] – through a unitary transformation of the band states – that the Hamiltonian (1) is equivalent to a two band Anderson model in which the first band does not interact with the QD, and the second is coupled to the quantum dot states through the hybridization $V = \sqrt{V_S^2 + V_D^2}$. Thus the problem of calculating the transport properties of Hamiltonian (1) is reduced to the problem of calculating the spectral properties of the one band Anderson model, provided that the actual lead-dot coupling strength is given by[28]

$$\Gamma = \Gamma_S + \Gamma_D = \pi N(\varepsilon_F)\, V^2, \quad (3)$$

where $N(\varepsilon_F)$ is the density of states (per spin) of the leads at the Fermi level, ε_F. It is reasonable to approximate the conduction bands of the leads with those of a non interacting two dimensional Fermi gas. Thus the density of states (DOS) per spin may be written as $N(\varepsilon) = 1/2D$, where D is one half of the band-width, therefore $\Gamma = \pi V^2/2D$.

The main difference between the Anderson model used in the ordinary Kondo problem and the one used here is the following. In the present model the energy difference $\varepsilon_0 - \varepsilon_F$ is not fixed, but, on the contrary, it can be tuned by a gate voltage V_g, coupled to the QD through a capacitor. From now on we set the Fermi level $\varepsilon_F = 0$. In first approximation, we can assume that $-\varepsilon_0$ increases linearly with eV_g (with common conventions for the sign of gate voltage). Thus the equilibrium thermodynamic properties of the system described by the Hamiltonian (1) are functions of two external parameters: the temperature T and the gate voltage V_g.

B. Linear response conductance

In the linear response regime ($V_{SD} \ll V_g$, where V_{SD} is the source-drain voltage), the conductance of the system QD+leads, G, may be written in a Landauer-like form[17,18]

$$\mathrm{G}(T, V_g) = \frac{2e^2}{h} \int_{-\infty}^{+\infty} \pi\Gamma \left(-\frac{1}{\pi} \mathrm{Im}\{G^R(\varepsilon + i\eta)\} \right) \left(-\frac{\partial f}{\partial \varepsilon} \right) \mathrm{d}\varepsilon, \quad (4)$$

where for simplicity we assume that the couplings to the leads are symmetric ($\Gamma_S = \Gamma_D$). Here f is the

Fermi distribution function and $G^R(\varepsilon + \mathrm{i}\eta)$ is the retarded local Green function, i.e. the Fourier transform of $G^R(t) \equiv -\mathrm{i}\Theta(t)\langle\{d(t), d^\dagger(0)\}\rangle$.

The quantity $\mathrm{Im}\left\{G^R(\varepsilon + \mathrm{i}\eta)\right\}$ in Eq. (4) is proportional to the local density of states, $\rho(\varepsilon)$, defined as

$$\rho(\varepsilon) \equiv -\frac{1}{\pi}\,\mathrm{Im}\left\{G^R(\varepsilon + \mathrm{i}\eta)\right\}. \tag{5}$$

We point out that the effects of the Coulomb interaction among electrons in the QD are contained in the local density of states. The main purpose of this work is thus to calculate $\rho(\varepsilon)$ as a function of temperature and gate voltage, and the resulting linear conductance.

C. Number of electrons

The low temperature transport properties of a mesoscopic system such as the QD+leads previously described are characterized by the phenomenon of charge quantization. When Coulomb blockade occurs the number of electrons in the QD is a fixed integer. This number can be changed by raising the voltage of the gate electrode. In this way the energy of the electrons in the QD is lowered with respect to the Fermi energy in the leads. The change in energy necessary to add a new electron is $\sim U$. This may be seen as the energy required to charge the QD, $e^2/2C$, where C is the capacitance of the QD. Thus the average number of electrons on the QD, $\langle n\rangle$, with

$$\langle n\rangle = N \int_{-\infty}^{+\infty} \mathrm{d}\varepsilon\, f(\varepsilon)\rho(\varepsilon), \tag{6}$$

is an important quantity in this problem (here N is the degeneracy of ε_0 and in the present case $N = 2$). The number of electrons is — like the conductance — a function of the local density of states.

D. Finite-U non-crossing approximation

In order to calculate $\rho(\varepsilon)$, the local DOS for the single impurity Anderson model, we adopt the finite-U non-crossing approximation (UNCA) approach,[27] an extension of the non-crossing approximation (NCA) to the finite U Anderson model. We point out that a finite U treatment is necessary in order to calculate the correct behavior of the conductance as a function of the gate voltage (and thus of the number of electrons on the QD).

The NCA is a diagrammatic technique introduced for the Anderson model in the $U \longrightarrow \infty$ limit.[24,25] The main idea of the NCA is that the self energy can be expanded in a series of diagrams of order V^2/N, where N is the degeneracy of the local level, usually large for Kondo impurities in diluted magnetic alloys (e.g. $N = 6$ for Ce impurities). The non-crossing diagrams are summed up to all orders, and the first neglected diagrams are of order $(V^2/N)^2$. The NCA was proved to be successful[29] already for $N = 2$. Thus it was applied with good results also to the spin-1/2 $U \to \infty$ Anderson model out of equilibrium,[19,20] e.g. it was used to calculate the behavior of the conductance as a function of the chemical potential in the QD+leads problem.

The NCA and the UNCA lead to a set of integral equations for the self energy, which have to be solved self-consistently. The number of equations depends on the number of many body states for the electrons in the QD. If U is finite there are four possible manybody states, namely $|0,0\rangle$ (with energy $\varepsilon = 0$), $|1,\downarrow\rangle$ and $|1,\uparrow\rangle$ (degenerate, with energy $\varepsilon = \varepsilon_0$), and $|2,\uparrow\downarrow\rangle$ (with energy $\varepsilon = 2\varepsilon_0 + U$). For each state a self energy and a ionic propagator are introduced. Thus we have three self energies, Σ_0, Σ_1, Σ_2 and three propagators, G_0, G_1, G_2 (due to spin degeneracy $G_{1\uparrow} = G_{1\downarrow} = G_1$ and $\Sigma_{1\uparrow} = \Sigma_{1\downarrow} = \Sigma_1$). The UNCA equations may then be written as[27,30]

$$\Sigma_0(\omega + \mathrm{i}\eta) = \frac{2\Gamma}{\pi}\int_{-D}^{D} \mathrm{d}\varepsilon\; f(\varepsilon)G_1(\omega + \varepsilon + \mathrm{i}\eta), \tag{7}$$

$$\Sigma_1(\omega + \mathrm{i}\eta) = \frac{\Gamma}{\pi}\int_{-D}^{D} \mathrm{d}\varepsilon\; [1 - f(\varepsilon)]G_0(\omega - \varepsilon + \mathrm{i}\eta) + \\ + \frac{\Gamma}{\pi}\int_{-D}^{D} \mathrm{d}\varepsilon\; f(\varepsilon)G_2(\omega + \varepsilon + \mathrm{i}\eta), \tag{8}$$

$$\Sigma_2(\omega + \mathrm{i}\eta) = \frac{2\Gamma}{\pi}\int_{-D}^{D} \mathrm{d}\varepsilon\; [1 - f(\varepsilon)]G_1(\omega - \varepsilon + \mathrm{i}\eta), \tag{9}$$

with

$$G_0(\omega + \mathrm{i}\eta) = \left[\omega + \mathrm{i}\eta - \Sigma_0(\omega + \mathrm{i}\eta)\right]^{-1}, \tag{10}$$

$$G_1(\omega + \mathrm{i}\eta) = \left[\omega + \mathrm{i}\eta - \varepsilon_0 - \Sigma_1(\omega + \mathrm{i}\eta)\right]^{-1}, \tag{11}$$

$$G_2(\omega + \mathrm{i}\eta) = \left[\omega + \mathrm{i}\eta - 2\varepsilon_0 - U - \Sigma_2(\omega + \mathrm{i}\eta)\right]^{-1}. \tag{12}$$

In the infinite U limit, the double occupation state is forbidden, and G_2 may be neglected.

Once this system of six equations is solved, it is possible to express all the physical quantities in terms of the ionic resolvents. In particular the retarded local Green function may be evaluated by analytic continuation from the corresponding imaginary time propagator, which may be written as[27]

$$G(\mathrm{i}\omega) = \frac{1}{Z}\oint_C \frac{\mathrm{d}z}{2\pi\mathrm{i}}\,\mathrm{e}^{-z/k_BT}\;\times \\ \left[G_0(z)G_1(z + \mathrm{i}\omega) + G_1(z)G_2(z + \mathrm{i}\omega)\right], \tag{13}$$

where Z is the QD partition function, i.e.

$$Z = \oint_C \frac{\mathrm{d}z}{2\pi\mathrm{i}}\,\mathrm{e}^{-z/k_BT}\;\left[G_0(z) + G_1(z) + G_2(z)\right] \tag{14}$$

Finally, the local density of states of the QD can be obtained from the retarded local Green function through Eq. (5).

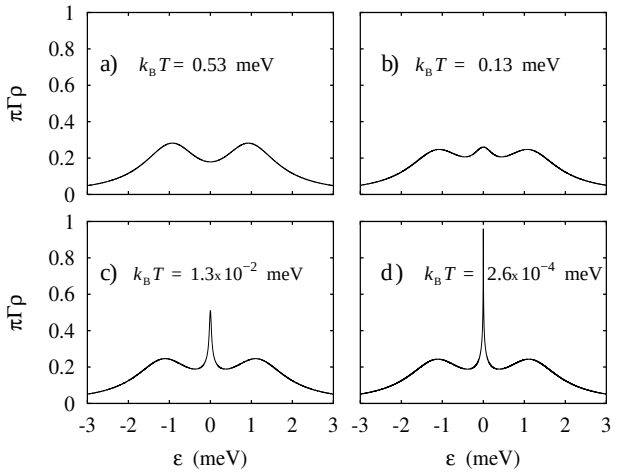

FIG. 1. Equilibrium density of states for the particle-hole symmetric Anderson model ($U = -2\varepsilon_0$) at different temperatures. Parameters: $\varepsilon_0 = -1$ meV, $U = 2$ meV, $\Gamma = 0.35$ meV, $D = 4$ meV. For $k_BT = 2.6 \times 10^{-4}$ meV ($T = 3$ mK) the local DOS at Fermi energy is $\pi\Gamma\rho(0) = 0.98$. In this paper the Fermi level ε_F is set equal to zero.

The NCA and the UNCA break down below a temperature T^*, which in the Kondo regime is much smaller than T_K.[24–27] Below this temperature spurious features show up, e.g., in the local density of states. It is known that the exact results are recovered with the inclusion of vertex corrections,[31–33] within a set of integral equations which are numerically heavier than Eqs. (7-12). This is, however, beyond the purpose of the present paper. Here we will use the UNCA without vertex diagrams. We will see that, nevertheless, we can reproduce fairly well both the high and low temperature regimes, and that (above T^*) the local DOS calculated with the UNCA is in good agreement with the exact numerical renormalization group (NRG) results.

III. NUMERICAL RESULTS

We solve the self-consistent UNCA equations, and calculate the local DOS, by using the fast Fourier transforms technique.[30] From $\rho(\varepsilon)$ we then obtain the Landauer conductance and the number of electrons as a function of the temperature and of the position of the QD level, ε_0, proportional to $-V_g$.

A. Local density of states

The local density of states is shown in Fig. 1 as a function of the energy. The ratio $-\varepsilon_0/\Gamma \sim 2.85 > 1$, and thus the model describes the system in the Kondo regime. For simplicity, we show the results for the particle-hole symmetric Anderson model ($U = -2\varepsilon_0$). The Kondo temperature may be estimated from Haldane formula,[34]

$$k_BT_K \sim (U\Gamma/2)^{1/2} \exp\left[\pi\varepsilon_0(\varepsilon_0+U)/(2U\Gamma)\right], \qquad (15)$$

and in the present case we find $k_BT_K \sim 0.06$ meV.

In the high temperature limit ($T \gg T_K$, Fig. 1a), the local density of states shows two broad resonances. The first one is located at energy $\varepsilon = E(n=1) - E(n=0) \equiv \varepsilon_0$, the energy required to put the first electron in the QD. The second resonance appears at $\varepsilon = E(n=2) - E(n=1) \equiv \varepsilon_0 + U$, the energy required to add an additional electron. The shape of the resonance peaks is Lorentzian. The origin of the peak broadening is mainly the coupling QD-leads measured by the width Γ, although a small thermal contribution is present since $k_BT \gtrsim \Gamma$.

As the temperature decreases, a peak – which is the fingerprint of the Kondo effect – appears close to the Fermi level. The height of the peak increases on decreasing the temperature. Figure 1 shows that for $T \ll T_K$ the height of the Kondo peak tends to a maximum value, i.e. $\pi\Gamma\rho(\varepsilon_F = 0) \longrightarrow 1$, which is reached exactly only at $T = 0$. At $k_BT = 2.6 \times 10^{-4}$ meV ($T/T_K \sim 0.01$, Fig. 1d) we find $\pi\Gamma\rho(0) \sim 0.98$.

The evolution of $\rho(\varepsilon)$ as a function of temperature is in fairly good agreement with the NRG results.[21,23,35] In the very large U limit we find results consistent with those obtained by using the NCA method with infinite U .[24,25]

B. Linear-response conductance

The linear response conductance G and the average number of electrons $\langle n \rangle$ are shown in Fig. 2 as a function of $-\varepsilon_0$.[36] For $-\varepsilon_0 < U/2$, when the number of electrons in the dot is $n \leq 1$, there are three relevant regimes of interest: the Kondo (K) regime $\Gamma < -\varepsilon_0 < U/2$, the mixed valence (MV) regime $|\varepsilon_0| < \Gamma$, and the empty orbital (EO) regime $-\varepsilon_0 < -\Gamma$. In the opposite case $-\varepsilon_0 > U/2$, when the number of electrons in the QD is $n \geq 1$, it is convenient to discuss the various regimes in terms of holes; thus the Kondo regime exists for $U/2 < -\varepsilon_0 < U - \Gamma$, the mixed valence regime for $|-\varepsilon_0 - U| < \Gamma$, and the empty orbital regime with $n \simeq 2$ occurs for $-\varepsilon_0 > U + \Gamma$. These regimes are schematically indicated in Fig. 2b.

In the Kondo regime, we can extimate the Kondo temperature from Haldane formula, Eq. (15). We find $k_BT_K \sim 10^{-5} - 10^{-2}$ meV for $\Gamma \sim 0.094$ (Fig. 2a) and $k_BT_K \sim 0.062 - 0.161$ meV for $\Gamma \sim 0.35$ (Fig. 2b).

Figure 2a shows the results obtained for $k_BT \sim 0.5\Gamma \gg k_BT_K$. In this limit it was shown[11,17] that the conductance has narrow peaks every time the average number of electrons in the QD increases by one. The peaks are separated by valleys in which the conductance is almost zero. This behavior (which is due to the Coulomb blockade[12]) is well reproduced in Fig. 2a. The peaks reach about

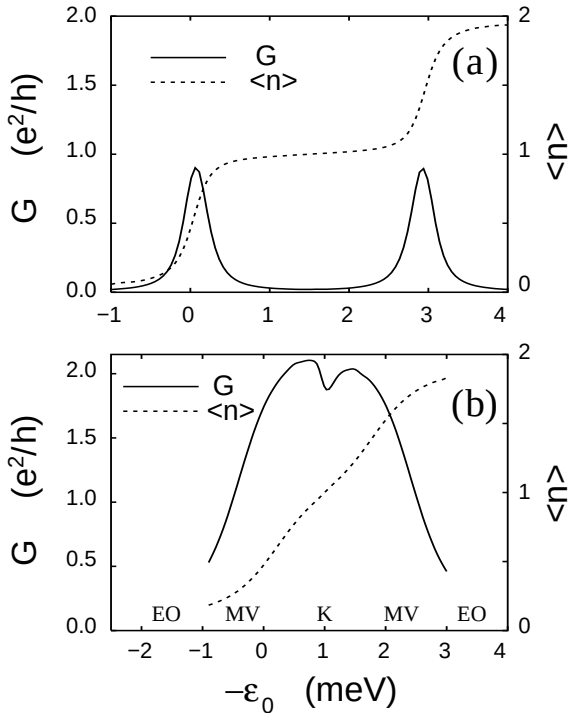

FIG. 2. Linear-response conductance G and average number of electrons on the dot $\langle n \rangle$, for two different set of parameters: (a) Parameters are: $\Gamma = 0.094$ meV, $D = 4$ meV, $U = 3$ meV, and $k_B T = 4.3 \times 10^{-2}$ meV ($T = 500$ mK) (Coulomb blockade); (b) Parameters are: $\Gamma = 0.35$ meV, $D = 4$ meV, $U = 2$ meV, and $k_B T = 4.3 \times 10^{-4}$ meV ($T = 5$ mK). The various regimes as a function of $-\varepsilon_0$ are schematically indicated in (b) (see text).

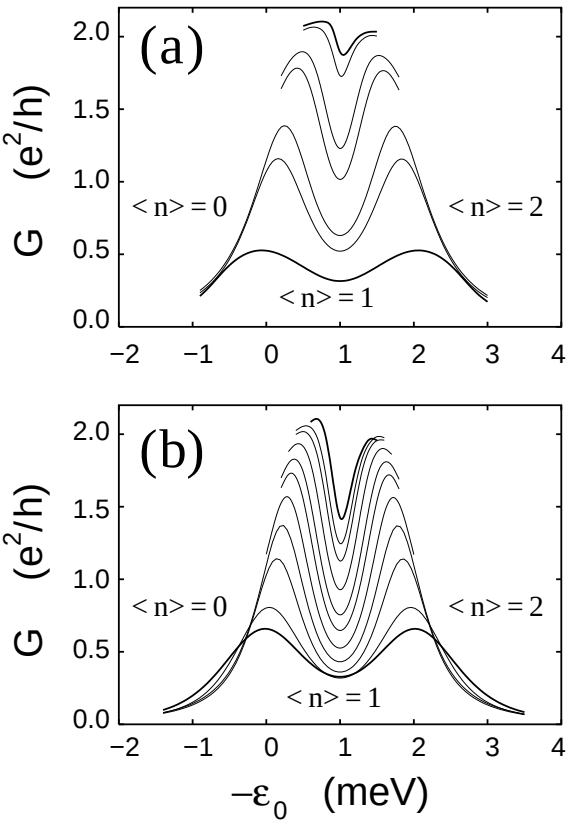

FIG. 3. Linear response conductance as a function of $-\varepsilon_0$ (ε_0 is always referred to the Fermi level, being $\varepsilon_F = 0$) the energy of the dot level with respect to the Fermi energy, and for many temperatures. (a) Parameters: $\Gamma = 0.35$ meV, $D = 4$ meV, $U = 2$ meV. Temperatures (from the bottom to the top curve): $k_B T = 0.43$, 0.086, 0.043, 8.6×10^{-3}, 4.3×10^{-3}, 8.6×10^{-4}, and 4.3×10^{-4} meV. (b) Parameters: $\Gamma = 0.275$ meV, $D = 4$ meV, $U = 2$ meV. Temperatures (from the bottom to the top curve): $k_B T = 0.26$, 0.17, 0.07, 0.035, 0.017, 8.6×10^{-3}, 5.3×10^{-3}, 2.6×10^{-3}, 1.3×10^{-3}, 8.6×10^{-4}, and 4.3×10^{-4} meV.

e^2/h, as expected from Coulomb blockade theory in the limit $k_B T \sim \Gamma$, and have a width of about 2Γ. This broadening is due to tunneling, while the thermal broadening is negligible. The line shape is almost Lorentzian. If the temperature is raised so much that $k_B T \gg \Gamma$ the height of the peaks becomes much smaller than e^2/h and their width is controlled by thermal broadening only.

Figure 2b shows G and $\langle n \rangle$ for $T \ll T_K$. In this regime, experiments[2–7] show that the valleys tend to raise when the number of electrons in the QD is odd, and remain almost unchanged when the number of electrons in the QD is even. In the very low temperature limit, the valleys with an odd number of electrons evolve into a plateau[7] at $G \sim 2e^2/h$. This behavior is the manifestation of the Kondo effect in the mesoscopic transport properties of the QD+leads system. Figure 2b shows that when $\langle n \rangle \sim 1$ the conductance calculated with the UNCA tends to $G = 2e^2/h$, while a valley appears for $\langle n \rangle \sim 0$ and $\langle n \rangle \sim 2$. Thus the Kondo regime is well described by the adopted method. The average number of electrons in Fig. 2b has a regular increase and does not have well defined plateaux as in Fig. 2a, due to the larger value of Γ.

Thus we have shown that the UNCA can describe well both the Coulomb blockade and the Kondo effect. The results can be compared with the exact NRG calculations.[21–23] Agreement is very good in the Kondo regime, down to $T \sim 0.01 T_K$. In the mixed valence and empty orbital regimes the agreement decreases. At low temperature the UNCA breaks down and a spurious peak appears in the local DOS, close to the Fermi level, as discussed for the usual NCA in Ref. 32. Within the parameters and the temperature chosen in Fig. 2b, this happens approximately for $-\varepsilon_0 < 0.5$ meV and $-\varepsilon_0 > 1.5$ meV. In this region the conductance calculated with the UNCA is much larger than the exact NRG result. Therefore from now on we will plot the conductance only for the values of T and ε_0 for which the UNCA is reliable.

The linear-response conductance is shown in Fig. 3 as a function of $-\varepsilon_0$ and for several different temperatures. The results are shown for two different choices

of the tunneling width: $\Gamma = 0.35$ meV (Fig. 3a) and $\Gamma = 0.275$ meV (Fig. 3b). In the Kondo regime, we estimate the Kondo temperature by using Haldane formula, and find $k_B T_K \sim 0.062 - 0.161$ meV for $\Gamma = 0.35$ meV and $k_B T_K \sim 0.030 - 0.134$ meV for $\Gamma = 0.275$ meV.

Figure 3a shows that at high temperature ($k_B T > \Gamma \gg k_B T_K$) there are two Coulomb blockade peaks at energy $-\varepsilon_0 \sim 0$ and $-\varepsilon_0 \sim U$, the maximum value of the conductance being $G \sim 0.5 e^2/h$. As the temperature decreases, the Coulomb blockade peaks become closer to each other, and ideally merge into a plateau at $T = 0$. This is due to the fact that the energy $-\varepsilon_0$ itself is renormalized by the many body effects, through the real part of the self energy. At very low temperature we see that $G \sim 2e^2/h$ (with maximum deviation of 10%) in the region in which the number of electrons is odd ($n \sim 1$).

The same behavior is shown in Fig. 3b. Here we choose a smaller value of Γ, so that the Kondo temperature is smaller. At high temperature we see again the two Coulomb blockade peaks, located at $-\varepsilon_0 \sim 0$ and $-\varepsilon_0 \sim U$. At very low temperature the peaks approach each other and tend to the maximum value $2e^2/h$. However in this case the deviation from the limiting value is larger (about 25%). This is due to the fact that, because of the smaller T_K, down at $T \sim 0.01 T_K$ (about the lowest temperature that can be reached before the UNCA breaks down) we have $\pi\Gamma\rho(0) \sim 0.75$ instead of $\pi\Gamma\rho(0) = 1$. Nevertheless, Fig. 3b reproduces the theoretical NRG calculations in the Kondo regime at several different temperatures, see e.g. Fig. 3 in Ref. 21, Fig. 2 in Ref. 22, and Fig. 2a of Ref. 23. In addition, at high temperature Fig. 3b provides very good results in the whole range of $-\varepsilon_0$.

It is worth to remind that when $k_B T > \Gamma$ the peak broadening is mainly due to thermal effects. Thus, when we start from the high temperature regime and lower the temperature, at first the peak width decreases. This effect is shown in Fig. 3b. On the contrary, when $k_B T \sim \Gamma$ the broadening is about 2Γ, in agreement with experimental results.[3,7] If the Kondo temperature is negligibly small, lowering the temperature below Γ/k_B does not produce any further change in the peak width. However, if the Kondo temperature is finite, as soon as $k_B T \sim k_B T_K \ll \Gamma$ the two peaks tend to become broader, and merge in a single large peak at zero temperature. This effect is shown in Fig. 3.

The UNCA results in Fig. 3 can be directly compared to the experimental measurements of the linear conductance vs the gate voltage. The curves in Fig. 3 reproduce very well the experiments described in Refs. 2–4,7, in which the measurement of the Kondo effect in the equilibrium conductance of a QD+leads system is reported. Agreement is satisfactory for the temperature dependence and the broadening of the peaks, and it covers the whole range of electron occupancy $0 \leq n \leq 2$.

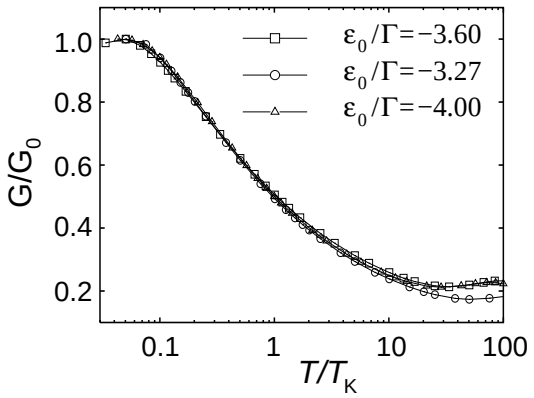

FIG. 4. Universal behavior of linear-response conductance normalized to its saturation value G_0. The conductance is displayed as a function of T/T_K, for three different values of ε_0/Γ chosen in the Kondo regime. Parameters: $\Gamma = 0.275$ meV, $D = 4$ meV, $U = 2$ meV.

IV. SCALING BEHAVIOR

In diluted magnetic alloys, the low temperature ($T \leq T_K$) resistivity, $\rho(T)$, follows a universal scaling law,[1,35] i.e. $\rho/\rho_0 = F(T/T_K)$, where $\rho_0 \equiv \rho(T = 0)$ and $F(x)$ is a function independent on system-related parameters. This happens because at low temperature and in the Kondo regime there is only one relevant energy scale, $k_B T_K$. Similar scaling properties have been reported for the low temperature conductance of QD devices,[3,7,9,10] and carbon nanotubes.[37] For a QD device described by the spin-1/2 Anderson model the universal function G/G_0 was recently calculated by using the NRG.[22] Here we calculate the same function by using the UNCA, and compare our results with the NRG calculations and experimental data.

A. Universal curves

The conductance calculated with the UNCA is shown in in Fig. 4 as a function of T/T_K. The different set of points correspond to different choices of $-\varepsilon_0/\Gamma$ in the Kondo regime ($-\varepsilon_0/\Gamma = 3.6$ corresponds to the particle-hole symmetric point, that is $-\varepsilon_0 = U/2 = 1$ meV in Fig. 3b). The conductance is normalized to $G_0 \equiv G(T_0, V_g)$, where T_0 is the lowest temperature which can be reached before the UNCA breaks down. In order to achieve a universal behavior we define the Kondo temperature such that $G(T_K) = G_0/2$, as often done.[3,7] The relative deviation from ideal result in the Kondo region for $-\varepsilon_0/\Gamma$, that is $\delta = (G_0 - 2e^2/h)/(2e^2/h)$, depends on the choice of the parameters (we find $2\% < |\delta| < 25\%$). Figure 4 shows that the conductance follows the universal behavior in a fairly large range of temperatures. Departures from this universality are observed only for $T \gg T_K$, as

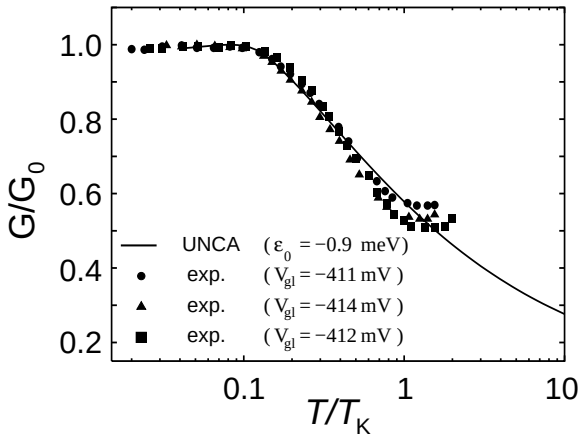

FIG. 5. Experimental data (Fig. 3c of Ref. 7) compared with the UNCA universal curve G/G_0. Parameters of the theoretical curve: $\varepsilon_0/\Gamma = -3.27$, $D = 4$ meV, $U = 2$ meV. Here V_{gl} is the gate voltage.[7]

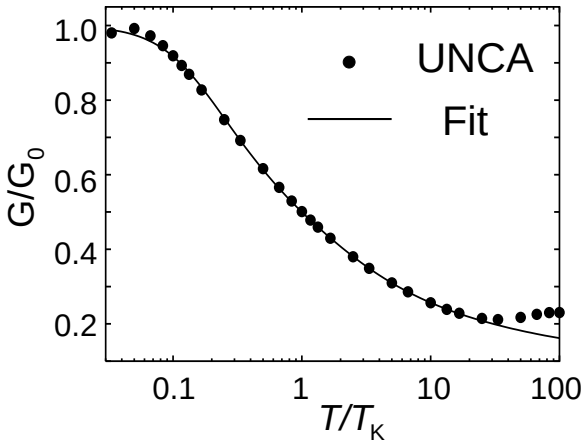

FIG. 6. Universal curve G/G_0 ($\varepsilon_0/\Gamma = -3.6$) compared with the interpolation function given in Eq. (19). The resulting fit parameters are: $a = 1/\ln(1+b+c) \simeq 0.25$, $b = 43.4$ and $c = 10.25$.

expected. We point out that at very low temperature ($T/T_K \ll 1$) the universal curve has the expected Fermi liquid behavior,[38] i.e. $(G-G_0)/G_0 \propto T^2$, while at higher temperature ($T/T_K \sim 1$) the conductance is proportional to $\ln(T/T_K)$.

The universal curve of the conductance calculated with the UNCA is similar to NRG results for the ordinary Kondo problem (see e.g. Fig. 4 of Ref. 3 or Fig. 12 of Ref. 35) and to NRG results for the conductance in QD devices (see Figs. 4 and 7a of Ref. 22).

B. Comparison with experiments

The universal curve calculated here can be directly compared with existing measurements of the conductance. In this section we will compare in particular with the experimental data taken from Ref. 7. In Fig. 5 we show G/G_0 vs T/T_K, and plot both the experimental points and our UNCA curve. In Ref. 7 the experimental data were normalized to G_0, the value of the conductance at the lowest temperature for which a measurement exists, and the Kondo temperature was defined as the temperature such that $G(T_K) = G_0/2$.

We found the best agreements between UNCA and experiments for the choice $\varepsilon_0/\Gamma = -3.27$. Figure 5 shows that the crossover from the logarithmic behavior to the low temperature Fermi liquid regime is reproduced fairly well by the conductance calculated by using the UNCA.

C. Interpolation formula

In order to extract the Kondo temperature from experimental data, it has become very common[3,7,37] to fit the data with the empirical formula

$$G(T) = G_0 \left(\frac{{T'_K}^2}{T^2 + {T'_K}^2} \right)^s \tag{16}$$

where $T'_K = T_K/\sqrt{2^{1/s}-1}$ and $G(T_K) = G_0/2$. This formula reproduces well NRG results for $T < T_K$ and has a single fitting parameter, s. However, in the intermediate temperatures regime ($T \sim T_K$) the exact conductance is proportional to $\ln(T/T_K)$, as NRG calculations show,[22] and this behavior is not explicitly accounted for in formula (16). Here we propose an alternative phenomenological formula, which (a) is still quite simple, (b) reproduces fairly well the calculated conductance in the whole temperature regime and (c) shows explicitly the logarithmic behavior in the intermediate temperature regime. Our formula has two fitting parameters instead of one.

We notice that at very low temperature, in the Fermi liquid regime ($T \ll T_K$), the conductance should show the Fermi liquid T^2 behavior,

$$G = G_0 \left(1 - \alpha \frac{T^2}{T_K^2} \right), \tag{17}$$

where α is a parameter. Instead, at higher temperatures ($T \sim T_K$) a logarithmic behavior is expected

$$G \propto G_0 \ln(T/T_K). \tag{18}$$

A function that satisfies both requirements is the following

$$\frac{G}{G_0} = \left(1 + a \ln \left[1 + b \left(\frac{T}{T_K} \right)^2 + c \left(\frac{T}{T_K} \right)^4 \right] \right)^{-1}, \tag{19}$$

where a, b, and c are dimensionless parameters to be determined with best fit techniques. By defining T_K

as the temperature such that $G(T_K) = G_0/2$, we find $a = 1/\ln(1 + b + c)$. Thus there are only two fitting parameters in our formula.

In Fig. 6 we show the results of a fit for the choice $-\varepsilon_0/\Gamma = -3.6$. The empirical formula reproduces extremely well the UNCA results for the values $b = 43.4$, $c = 10.25$. These parameters slightly depend, of course, on the choice of $-\varepsilon_0/\Gamma$, and of the other UNCA parameters. Thus Eq. (19) reproduces the correct behavior, and it is physically correct both in the $T \ll T_K$ and $T \sim T_K$ regime. We notice that the fourth order term is required to reproduce the behavior of the conductance in the intermediate temperature regime, while the T^2 term is required to reproduce the low temperature Fermi liquid behavior.

V. CONCLUSION

In the present work we have calculated the conductance of a system made of a quantum dot coupled to two leads, described by the spin-1/2 Anderson model. We adopted the finite-U non-crossing approximation method (UNCA), which allowed us to calculate the conductance for the Anderson model with finite Coulomb repulsion. Thus we were able to study the conductance as a function of temperature and gate voltage. We have shown that the results obtained with this method are in good agreement with those obtained by using the exact numerical renormalization group (NRG).[21–23] In addition we reproduced both the Coulomb blockade and the Kondo effect in quantum dots. Inclusion of a finite Coulomb correlation is important in order to describe correctly the experimental results in the whole regime of electron occupancies. The comparison with experimental data of Ref. 7 is fairly good, for what concerns both temperature and gate voltage dependence. Finally we have suggested a simple phenomenological formula which fits UNCA results both in the logarithmic and in the Fermi-liquid temperature regions, reproducing very well also the crossover between them.

Although the spin-1/2 Anderson model can be solved by using the exact NRG, we believe that the UNCA is more suitable than NRG for extension to realistic systems, e.g. for taking into account the effects of the electronic structure of the dots, and thus we point out that the UNCA method can become an important tool to interpret the experiments. Possible applications are, for example, in the explanation of the Kondo effect in quantum dots for integer spin[9] and the Kondo effect in carbon nanotubes.[37]

ACKNOWLEDGMENTS

We would like to thank S. De Franceschi for helpful discussions and for a critical reading of the manuscript, and J. Schmalian for useful correspondence concerning his UNCA code. The numerical calculations were partly performed at the Computing Center of Collegio Borromeo in Pavia, whose support is gratefully acknowledged.

[1] A. C. Hewson, *The Kondo Problem to Heavy Fermions*, Cambridge University Press (1993).
[2] D. Goldhaber-Gordon, H. Shtrikman, D. Mahalu, D. Abusch-Magder, U. Meirav, and M. A. Kastner, Nature **391**, 156 (1998).
[3] D. Goldhaber-Gordon, J. Göres, M. A. Kastner, H. Shtrikman, D. Mahalu, and U. Meirav, Phys. Rev. Lett. **81**, 5225 (1998).
[4] S. M. Cronenwett, T. H. Oosterkamp, and L. P. Kouwenhoven, Science **281**, 540 (1998).
[5] J. Schmid, J. Weis, K. Eberl, and K. von Klitzing, Physica B **256 − 258**, 182 (1998).
[6] F. Simmel, R. H. Blick, J. P. Kotthaus, W. Wegscheider, and M. Bichler, Phys. Rev. Lett. **83**, 804 (1999).
[7] W. G. van der Wiel, S. De Franceschi, T. Fujisawa, J. M. Elzerman, S. Tarucha, and L. P. Kouwenhoven, Science **289**, 2105 (2000).
[8] J. Schmid, J. Weis, K. Eberl, and K. von Klitzing, Phys. Rev. Lett. **84**, 5824 (2000).
[9] S. Sasaki, S. De Franceschi, J. M. Elzerman, W. G. van der Wiel, M. Eto, S. Tarucha, and L. P. Kouwenhoven, Nature **405**, 764 (2000).
[10] L. P. Kouwenhoven and L. I. Glazman, Physics World **14**, 33 (January 2001)
[11] C. W. J. Beenakker, Phys. Rev. B **44**, 1646 (1991).
[12] For a review see U. Meirav and E. B. Foxman, Semincond. Sci. Technol. **11**, 255 (1996); L. P. Kouwenhoven, C. M. Marcus, P. L. McEuen, S. Tarucha, R. M. Westervelt, and N. S. Wingreen, in *Mesoscopic Electron Transport*, Vol. 345 of NATO ASI Series E, edited by L. L. Sohn, L. P. Kouwenhoven, and G. Schön (Kluwer Academic Publishers, 1997).
[13] P. W. Anderson, Phys. Rev. **124**, 41 (1961).
[14] T. K. Ng and P. A. Lee, Phys. Rev. Lett. **61**, 1768 (1988).
[15] L. I. Glazman and M. É. Raĭkh, JETP Lett. **47**, 452 (1988).
[16] A. Kawabata, J. Phys. Soc. Jpn. **60**, 3222 (1991).
[17] Y. Meir, N. S. Wingreen, and P. A. Lee, Phys. Rev. Lett. **66**, 3048 (1991).
[18] Y. Meir and N. S. Wingreen, Phys. Rev. Lett. **68**, 2512 (1992).
[19] Y. Meir, N. S. Wingreen, and P. A. Lee, Phys. Rev. Lett. **70**, 2601 (1993).
[20] N. S. Wingreen and Y. Meir, Phys. Rev. B **49**, 11040 (1994).
[21] W. Izumida, O. Sakai, and Y. Shimizu, J. Phys. Soc. Jpn. **67**, 2444 (1998).
[22] W. Izumida, O. Sakai, and S. Suzuki, J. Phys. Soc. Jpn. **70**, 1045 (2001).
[23] T. A. Costi, cond-mat/0103517, preprint (2001).
[24] N. E. Bickers, D. L. Cox, and J. W. Wilkins, Phys. Rev. B **36**, 2036 (1987).

[25] N. E. Bickers, Rev. Mod. Phys. **59**, 845 (1987).
[26] R. Monnier, L. Degiorgi, and B. Delley, Phys. Rev. B **41**, 573 (1990).
[27] T. Pruschke and N. Grewe, Z. Phys. B **74**, 439 (1989).
[28] The definition of Γ given in the present paper is the same adopted in Ref. 15. This definition differs from the one given in Refs. 17–20 by a factor of 2.
[29] D. L. Cox, Phys. Rev. B **35**, 4561 (1987)
[30] P. Lombardo, M. Avignon, J. Schmalian, and K. H. Bennemann, Phys. Rev. B **54**, 5317 (1996).
[31] F. B. Anders, J. Phys. Condens. Matter **7**, 2801 (1995).
[32] T. A. Costi, J. Kroha, and P. Wölfle, Phys. Rev. B **53**, 1850 (1996).
[33] K. Haule, S. Kirchner, J. Kroha, and P. Wölfle, Phys. Rev. B **64**, 155111 (2001).
[34] F. D. M. Haldane, Phys. Rev. Lett. **40**, 416 (1978).
[35] T. A. Costi, A. C. Hewson, and V. Zlatić, J. Phys. Condens. Matter **6**, 2519 (1994).
[36] Expressing the results as function of $-\varepsilon_0$, with ε_F set equal to zero, is equivalent to plotting the same curves as function of chemical potential at fixed ε_0 (see e.g. Fig. 6 of Ref. 20).
[37] J. Nygård, D. H. Cobden, and P. E. Lindelof, Nature **408**, 342 (2000).
[38] A. Kaminski, Yu. V. Nazarov, and L. I. Glazman, Phys. Rev. B **62**, 8154 (2000).